Ground and excited electronic states of azobenzene: A quantum Monte Carlo study

M. Dubecký,[1] R. Derian,[1] L. Mitas,[2] and I. Štich[1,a)]
[1]*Institute of Physics, CCMS, Slovak Academy of Sciences, 84511 Bratislava, Slovakia*
[2]*North Carolina State University, Department of Physics, Raleigh, North Carolina 27695, USA*

(Received 18 August 2010; accepted 6 October 2010; published online 22 December 2010; corrected 30 December 2010)

Large–scale quantum Monte Carlo (QMC) calculations of ground and excited singlet states of both conformers of azobenzene are presented. Remarkable accuracy is achieved by combining medium accuracy quantum chemistry methods with QMC. The results not only reproduce measured values with chemical accuracy but the accuracy is sufficient to identify part of experimental results which appear to be biased. Novel analysis of nodal surface structure yields new insights and control over their convergence, providing boost to the chemical accuracy electronic structure methods of large molecular systems. © *2010 American Institute of Physics*. [doi:10.1063/1.3506028]

Azobenzene (AB), $C_{12}H_{10}N_2$ (see Fig. 1) is an iconic photoswitchable molecule with a fairly simple molecular structure. AB exists in two different structural isomers, trans (*E*) and cis (*Z*), and the two isomers exhibit different physical properties and absorption bands which make AB a good candidate for light-triggered switches, image storage devices, and materials with photomodulable properties.[1,2] Laser light of appropriate wavelength[1,2] induces $E \rightleftharpoons Z$ photoswitching in AB, and in the ground state, S_0, isomerization can take place also thermally.[1,2] Besides these straightforward qualitative facts the photochemistry of AB is far from complete, both in theoretical understanding of quantum effects involved and also in accurate spectral data from experiments.

In this paper we focus on two main goals. First, we show that a balanced combination of standard quantum chemical basis set methods with fully correlated quantum Monte Carlo (QMC) approaches may be tuned to provide results with unprecedented accuracy applicable to large molecular systems. Second, this combination of methods enables us to introduce novel characterization of structure and convergence properties of many-body wave functions nodal hypersurfaces. As it is well-known, accuracy of the fixed-node QMC calculations is determined by the quality of the nodes. We demonstrate that the presented developments open up a route to treatment of both ground- and excited-state electronic structure of large molecular systems deemed beyond practical feasibility.

Experimentally, AB low-energy absorption spectra have been measured for isomers in both gas phase[3] and inert solvents.[4–6] The absorption spectra show peaks attributed to lowest singlet states of $n\pi^\star$ (S_1) and $\pi\pi^\star$ (S_2) type. However, they often correspond to forbidden or very small oscillator strength transitions and hence provide very weak signals leading to large differences of the order of few tens of an electron-volt which cannot be explained simply as a solvent effect. For example, the difference in the experimental $\epsilon^E_{S_0\rightarrow S_2}$ absorption peak in gas phase and solvent is ~0.2 eV and in $\epsilon^Z_{S_0\rightarrow S_2}$ even ~0.4 eV. Furthermore, the effect of the solvent should lead to an increase in the excitation energies of the $n\pi^\star$ states,[7] whereas the opposite is true for the experimental $\epsilon^Z_{S_0\rightarrow S_1}$ absorption, which is ~0.1 eV lower in solvent.

In such a situation accurate theoretical description is called to resolve the experimental uncertainties. However, the size of the molecule with almost hundred electrons precludes use of highly correlated quantum chemistry methods.[8] Conceptually the simplest approach used is based on the Density Functional Theory (DFT) generalized restricted open shell Kohn–Sham (gROKS) description of the lowest excited singlet state S_1.[9–12] The best quantum chemistry results up to date use CC2 (Ref. 13) and CAS–SCF/CAS–PT2 description.[14–16] The CAS–SCF/CAS–PT2 results will be used as benchmarks for comparison with our QMC results. While use of these methods provides very useful insights into dynamics of AB (Refs. 9–12, 17, and 18) or possible conical intersections, photo-isomerization pathways, quantum yields, etc.,[14–16,19,20] the medium accuracy of electronic correlations treatment by all these methods significantly limits the predictive power of the obtained results.

Due to its favorable low-order polynomial scaling with the system size, the QMC method[21,22] provides a practical route to achieving chemical accuracy for the system at hand. Most of the QMC applications up to date are restricted to ground states, with excited states still representing a direction with fairly little expertise.[23–27] Previous applications which combine determinantal expansions and QMC either deal with very small systems,[24–27] where highly correlated quantum chemistry calculations of similar accuracy exist or deal with systems of comparable size to AB but do not consider the multireference character of accurate wave functions.[23]

The accuracy of QMC calculations for large systems is determined by the accuracy of fermion nodes of the trial wave functions, and the so-called fixed-node approximation appears as both fundamentally and practically important barrier in this respect.[21,22] The key goal of our work is to overcome the fixed-node bias for both ground and excited

a)Author to whom correspondence should be addressed. Electronic mail: ivan.stich@savba.sk.

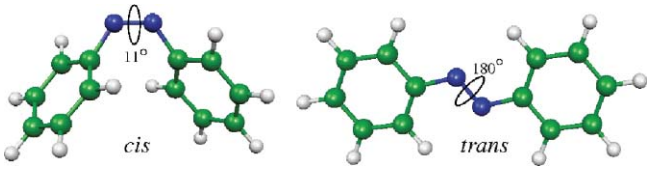

FIG. 1. Structure of trans and cis isomers of azobenzene. The circles highlight the CNNC dihedral angles.

states in large molecular systems which are out of reach of more traditional correlated methods based on basis sets. We combine medium accuracy quantum chemistry method, namely, CAS–SCF which includes only the key one-particle states, with a fully correlated variational Monte Carlo (VMC) and diffusion Monte Carlo (DMC) methods. We explicitly demonstrate and quantify a rapid convergence of the nodal surfaces for wave functions built from truncated CAS–SCF expansions combined with explicit Jastrow interparticle correlations. The quality of obtained results is remarkably high and enables to confirm the experiments within chemical accuracy, and, in addition, the predictions are reliable enough to identify experimental values which appear to be biased by experimental data analysis limits. The reoptimized CAS–SCF expansions with comparatively small number of determinants enable very effective and accurate description of the nodal surfaces. Hence, the CAS–SCF/QMC combination of methods ideally balances the relative strengths of both methods and therefore boosts the reach of chemical accuracy electronic structure calculations by an order of magnitude or more.

Four levels of modeling are used. For DFT and CAS–SCF we use the GAMESS suite of codes,[28,29] while all VMC and DMC calculations use the QWalk code.[30] All energies were calculated along the torsion coordinate (CNNC dihedral angle), which was shown to be the preferred pathway for both photo- and thermal isomerization processes.[15,16] The dihedral angle CNNC was increased in steps of ~10° with C_2 symmetry imposed. The ground-state geometries were calculated using DFT techniques with B3LYP xc-functional[31,32] with the Greeff–Lester type of effective core pseudopotential[33,34] for all species and cc-pVTZ basis set.[35] For the *E* isomer, where electron diffraction experiment exists,[36] the B3LYP geometries lie within experimental error bars. The active space in the CAS–SCF calculations was 14 electrons in 12 orbitals (14/12),[14–16] which corresponds to 10/10 π valence electrons and two doubly occupied nitrogen lone pairs. From CAS–SCF wave function, with orbital space individually tuned for each geometry, natural orbitals and expansion coefficients are generated. Subsequently a truncated CAS–SCF expansion is used retaining all determinants with weights $\geq$0.03 to construct the variational wave function with correlations explicitly built in via Schmidt–Moskowitz Jastrow factor,[22,37] including electron–electron, electron–nucleus, and electron–electron–nucleus correlations. Instead of Slater determinants we work with symmetry adapted configuration state functions (CSFs). The expansions consist of between 107 and 499 Slater determinants or 38 and 78 CSFs. The VMC trial wave function[22] and their nodes are optimized by minimizing variance and/or linear combination of energy and variance.[38] Final results are obtained by DMC runs.

TABLE I. Comparison of vertical $S_0 \rightarrow S_1$ excitation energies for trans isomer, $\epsilon^E_{S_0\rightarrow S_1}$, cis isomer, $\epsilon^Z_{S_0\rightarrow S_1}$, energy differences between *E* and *Z* isomer ground states, $\Delta E^{E-Z}_{S_0}$, and energies of transition state, $\Delta E^{TS}_{S_0}$, on the S_0 surface calculated using various methods; upper block: present results, middle block: results of previous calculations, bottom block: experimental results. CAS–SCF$_{opt}$ refers to calculations, where the active spaces are individually tuned for the given geometry, whereas CAS–SCF retains the same active space along the entire torsion coordinate. All energies in electronvolts, relative to *E* conformer.[a]

Method	$\epsilon^E_{S_0\rightarrow S_1}$	$\epsilon^Z_{S_0\rightarrow S_1}$	$\Delta E^{E-Z}_{S_0}$	$\Delta E^{TS}_{S_0}$
DFT(B3LYP)[b]	—	—	0.66	2.12
CAS–SCF[b]	3.22	3.35	0.66	2.25
CAS–SCF$_{opt}$[b]	3.10	3.27	0.73	2.04
DMC	2.82(6)	3.13(6)	0.50(6)	1.80(6)
gROKS(PBE)[c] (Refs. 10 and 11)	2.17	2.26	0.55	1.74
DFT(B3LYP)[d] (Ref. 14)	—	—	0.66	2.14
CAS–SCF[d] (Refs. 15 and 16)	3.18	3.38	0.71	1.80
CAS–PT2[d] (Refs. 15 and 16)	2.50	2.71	0.52	1.65
Expt. (gas phase) (Ref. 3)	2.82	2.92	—	1.73*
Expt. (in solvent) (Ref. 5)	2.88	2.88	—	—
Expt. (in solvent) (Ref. 39)	—	—	0.51	—

[a]Assuming $\Delta E^{E-Z}_{S_0} = 0.51$ eV (Ref. 39).
[b]cc-pVTZ basis.
[c]Plane-wave basis.
[d]6-31G* basis.

The main results are reported and compared with experiments and related previous calculations in Table I and Fig. 2. We find that all DFT results describe fairly well both minima on the S_0 surface. However, the barrier height at the transition state (TS), $\Delta E^{TS}_{S_0}$, which involves a complicated state formed by cleavage of a π-bond in the N=N group to form a biradical intermediate, appears to be strongly dependent on the xc-functional, with Perdew-Burke-Ernzerhof (PBE) functional (Refs. 40 and 41) providing significantly better results[10,11] than the B3LYP functional[14] by about

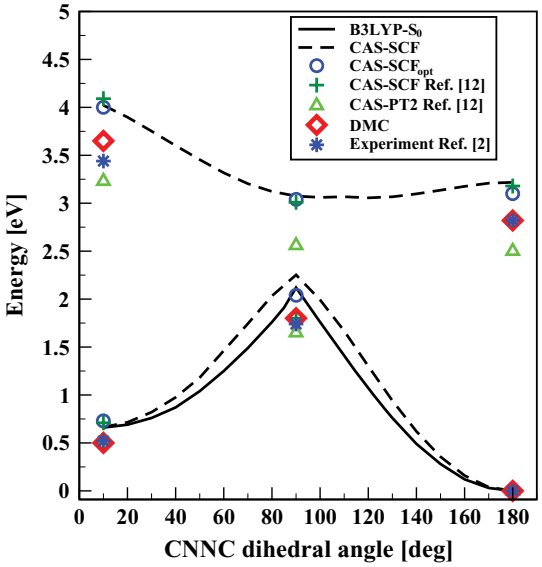

FIG. 2. Computed energies for S_0 and S_1 potential energy surfaces along the torsion coordinate compared to results of previous calculations (Refs. 15 and 16) and experiments (Ref. 3). In QMC results the error bars are smaller than the size of the points. All energies in electronvolts, relative to *E* conformer.

~0.4 eV. The differences between the present and previous B3LYP results[14] reflect mainly differences in the basis sets used. However, when it comes to the excited states the results worsen considerably. The gROKS method underestimates the excitations by as much as ~0.7 eV.[10–12] Our CAS–SCF results essentially reproduce the previous CAS–SCF results[15,16] by overestimating the excitations by ~0.4 eV, while our individually optimized CAS–SCF results are marginally better presumably due to slightly better basis sets used (cc–pVTZ versus 6–31G*). As can be seen, even the perturbationally corrected CAS–PT2 results[15,16] still exhibit significant errors by underestimating the excitations by up to 0.3 eV with respect to the gas-phase experiments.[3] We note that we do not attempt any comparison of the excitation energies with the experiments in solvents,[4–6] as equal values of vertical excitation energies for both conformers found in experiments in solvents, see Table I, are in disagreement with gas-phase experiments[3] as well as with all theoretical results.[9–11,13–16]

The *dramatic improvement* achieved with combination of CAS–SCF with QMC can clearly be seen in Table I and Fig. 2. $\epsilon^{E}_{S_0\to S_1}$, $\Delta E^{E-Z}_{S_0}$ are indistinguishable from the relevant experiments.[3,39] $\Delta E^{TS}_{S_0}$ shows only marginal difference of ~0.07 eV compared to the gas-phase experiment.[3] There are two possible sources for this difference. In our calculations the TS has been fixed to dihedral angle of 90°, whereas the real value may be slightly different. For instance, CAS–SCF results[15,16] found a value of 85°. Furthermore, a nonadiabatic $S_0 \to T_1 \to S_0$ torsion pathway via first excited triplet state, T_1, which crosses the S_0 potential energy surface (PES) was proposed.[15,16] Hence, the only deviation from the gas–phase experiment[3] of ~0.2 eV is found in $\epsilon^{Z}_{S_0\to S_1}$. The larger theoretical value of $\epsilon^{Z}_{S_0\to S_1}$ indicates that the S_1 PES is more curved, at least in the excitation part, than inferred from experiments. We note in passing that the experiment on the Z conformer may be laden with significant biases. The $S_0 \to S_1$ transition has not only a small oscillator strength[15,16] but the Z corresponding part of experimental data was reconstructed from very low intensity difference spectra using model parameters.[3]

In order to distinguish between possible experimental/theoretical biases, we now provide estimates of possible QMC errors. Essentially only three types of possible error may enter our QMC results: (1) DFT ground-state geometries, (2) nonlocality pseudopotential error, and (3) fixed-node error. A DFT test of sensitivity to geometries has been carried out in order to, at least indirectly, probe for the possible influence of point (1). Therefore we have compared B3LYP/PBE single point energies of isomers with PBE/B3LYP optimized geometries. In all cases the differences are of ~0.04 eV which is also consistent with the accurate result for calculated $\Delta E^{E-Z}_{S_0}$. The pseudopotential nonlocality error (2) is expected to be very similar for both isomers, as variational wave functions were converged to identical tolerance and variance. The nodal error (3) needs more consideration.

In order to quantify the quality and convergence of the nodal surfaces we have tested the following procedure. First, one needs to evaluate a difference between any two nodal surfaces, which can be done using the notion of Haussdorf distance.[42] However, this leads to a single number and does not reveal anything about the distribution of the differences and their change, e.g., during the optimizations. Therefore we found much more useful to measure the distribution of the differences. We choose a set of VMC configurations from the reference wave function, and for each configuration we identify a closest point on the nodal hypersurface by following the steepest descent path. For each walker we then find the distance of the closest point on the second wave function node in the normal direction, see Fig. 3. The distribution of such distances is then estimated by binning. Such an analysis, in spirit similar to ideas of Reboredo and Kent,[43] has not been applied to a real system before. As an example we show in Fig. 4 convergence of distribution of differences of VMC optimized nodal surfaces with respect

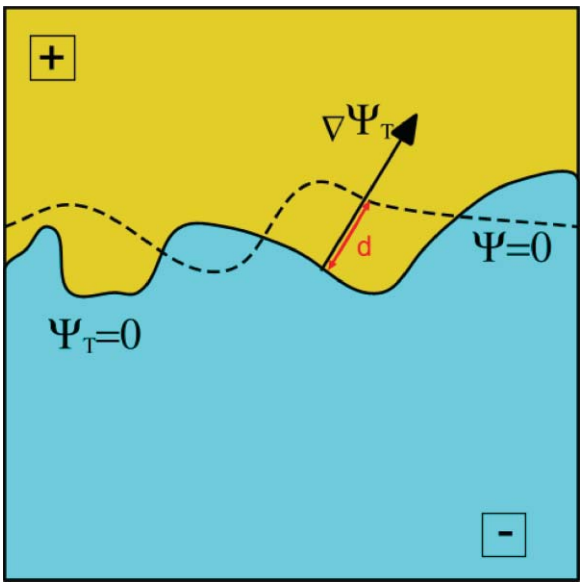

FIG. 3. Schematics of definition of the difference d between "reference" and "approximate" nodal surfaces.

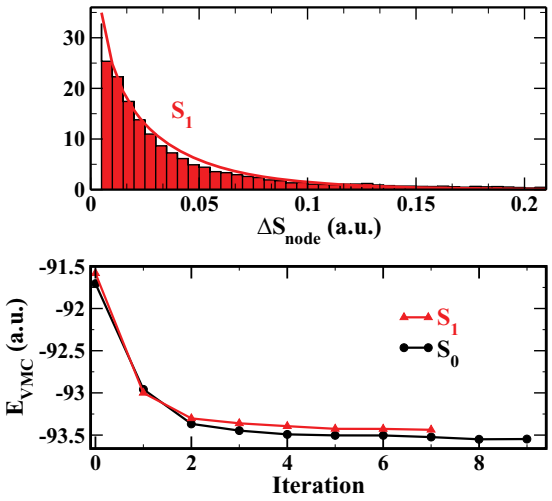

FIG. 4. Convergence of S_1 nodal surface and VMC energies for the E isomer. Upper panel: Distribution of the differences ΔS_{node} of the final VMC optimized S_1 nodal surface from the initial CAS–SCF surface. Lower panel: Convergence of S_0 (black) and S_1 (red) VMC energies.

TABLE II. Errors of CAS–SCF and DFT nodal surfaces for the E isomer characterized by the fall-off coefficient ξ_1 of the distribution of differences in nodal surfaces, ΔS_{node}, and in energy due to convergence of the nodes, ΔE_{node}. For details, see the text.

	ξ_1 (a.u.)		ΔE_{node} (eV)	
Method	S_0	S_1	S_0	S_1
DFT (B3LYP)	12.3	—	0.38(6)	—
CAS–SCF	33.1	21.8	<0.01	0.16(6)

to the CAS–SCF nodal surface, ΔS_{node}, for the S_1 state of the E isomer along with convergence of VMC energies of both S_0 and S_1 states. Another direct measure of the quality of the nodal surfaces is provided by comparison of energies due to nodal surface convergence. For that purpose we fix the parameters in the Jastrow factor to the final converged values and consider nodal surfaces corresponding to the different VMC iterations or methods. Representative DMC results are reported in Table II. For S_0 VMC optimization of the CAS–SCF nodal surface yields only negligible energy improvement. Improvements to the CAS–SCF nodal surface are more important for the S_1 state, where ≈0.16 eV can be gained by VMC optimization of the nodal surface. For comparison we report in Table II also values for DFT nodal surface. The comparison shows that a considerable error of ≈0.4 eV would result from use of the DFT nodal surface even in the ground state. In Table II we also report the values of the parameter ξ_1 in the fitting function $y = \xi_0 \exp(-\xi_1 x)/\sqrt[3]{x}$ characterizing the rate of fall-off of the distribution of the differences from the converged VMC nodal surface, see also Fig. 4. As an empirical observation, we find that $\xi_1 \approx 30$ introduces only negligible nodal error, $\xi_1 \approx 20$ requires a couple of iterations to reduce energy differences errors below chemical accuracy, and $\xi_1 \approx 10$ a significant nodal bias being present. For our system this implies that starting from CAS–SCF nodal surface the nodal errors beyond the second VMC iteration are negligible and that remaining energy decrease is only due to the "bosonic" correlation captured by the Jastrow factor,[22,37] see Fig. 4. Hence, the truncated CAS–SCF nodal surface represents an excellent and rapidly convergent starting point for a further VMC optimization and all computed energies are converged well below chemical accuracy.

We expect that for different systems the particular value of the ξ_1 coefficient may vary and several calculations with increasing variational freedom will be necessary to find the nodal hypersurface convergence. However, to the best of our knowledge, this is the first attempt to quantify the convergence of nodal hypersurfaces in a systematic manner.

In summary, a combination of CAS–SCF and QMC methods which ideally balances their relative strengths, augmented by techniques for analysis of structure and convergence control of nodal surfaces, was used to calculate ground and excited states of azobenzene, a large molecular system of technological importance. Remarkable accuracy achieved makes it possible not only to confirm experimental results with chemical accuracy but also to identify possible inaccuracies in part of the experimental data which, we believe, result from experimental data processing. The access to the properties of the nodal surfaces along with the control over their convergence can be used to boost efficiency of chemical accuracy electronic structure calculation well beyond the present day standards.[44] Work on the lowest triplet states, higher singlet states, and selected conical intersections is now under way.[44]

Financial support from APVV projects APVV-0091-07, LPP-0252-07 as well as Grant Nos. NSF DMR-0804549 and OCI-0904794 and ARO support are gratefully acknowledged. We acknowledge also the allocation at the NSF TACC center. This research was supported in part also by ERDF OP R&D, Project CE QUTE ITMS 26240120009, and via CE SAS QUTE. R.D. thanks M. Bajdich for valuable discussion on QMC and QWalk code. M.D. is grateful to P. M. Polestshuk for advice on construction of active space and fruitful discussions.

[1] H. Rau, in *Molecules and Systems*, edited by H. Dürr and H. Bouas-Laurent (Elsevier, Amsterdam, 1990).
[2] *Molecular Switches*, edited by B. L. Feringa (Wiley–VCH, Weinheim, 2001).
[3] J.-Å. Andersson, R. Petterson, and L. Tegnér, J. Photochem. **20**, 17 (1982).
[4] H. Rau, Angew. Chem. Int. Ed. Engl. **12**, 224 (1973).
[5] P. Hamm, S. M. Ohline, and W. Zinth, J. Chem. Phys. **106**, 519 (1997).
[6] I. K. Lednev, T.-Q. Ye, R. E. Hester, and J. N. Moore, J. Phys. Chem. **100**, 13338 (1996).
[7] M. Klessinger and J. Michl, *Excited States and Photochemistry of Organic Molecules* (VCH, Weinheim, 1993).
[8] A. Szabo and N. Ostlund, *Modern Quantum Chemistry: Introduction to Advanced Electronic Structure Theory* (Dover, New York, 1996).
[9] C. Nonnenberg, H. Gaub, and I. Frank, ChemPhysChem **7**, 1455 (2006).
[10] R. Turanský, M. Konôpka, N. L. Doltsinis, I. Štich, and D. Marx, ChemPhysChem **11**, 345 (2010).
[11] R. Turanský, M. Konôpka, N. L. Doltsinis, I. Štich, and D. Marx, Phys. Chem. Chem. Phys. **12**(42) 13853 (2010).
[12] M. Böckmann, N. L. Doltsinis, and D. Marx, J. Phys. Chem. A **114**, 745 (2010).
[13] H. Fliegl, A. Köhn, C. Hättig, and R. Ahlrichs, J. Am. Chem. Soc. **125**, 9821 (2003).
[14] L. Gagliardi, G. Orlandi, F. Bernardi, A. Cembran, and M. Garavelli, Theor. Chem. Acc. **111**, 363 (2004).
[15] A. Cembran, F. Bernardi, M. Garavelli, L. Gagliardi, and G. Orlandi, J. Am. Chem. Soc. **126**, 3234 (2004).
[16] I. Conti, M. Garavelli, and G. Orlandi, J. Am. Chem. Soc. **130**, 5216 (2008).
[17] T. Schultz, J. Quenneville, B. Levine, A. Toniolo, T. J. Martínez, S. Lochbrunner, M. Schmitt, J. P. Shaffer, and M. Z. Zgierski, and A. Stolow, J. Am. Chem. Soc. **125**, 8098 (2003).
[18] A. Toniolo, C. Ciminelli, M. Persico, and T. J. Martínez, J. Chem. Phys. **123**, 234308 (2005).
[19] T. Ishikawa, T. Noro, and T. Shoda, J. Chem. Phys. **115**, 7503 (2001).
[20] L. Wang, W. Xu, C. Yi, and X. Wang, J. Mol. Graphics Modell. **27**, 792 (2009).
[21] W. M. C. Foulkes, L. Mitas, R. J. Needs, and G. Rajagopal, Rev. Mod. Phys. **73**, 33 (2001).
[22] M. Bajdich and L. Mitas, Acta Phys. Slovaca **59**, 81 (2009).
[23] A. Aspuru-Guzik, O. E. Akramine, J. C. Grossman, and W. A. Lester, Jr., J. Chem. Phys. **120**, 3049 (2004).
[24] F. Schautz and C. Filippi, J. Chem. Phys. **120**, 10931 (2004).
[25] F. Schautz, F. Buda, and C. Filippi, J. Chem. Phys. **121**, 5836 (2004).
[26] P. M. Zimmerman, J. Toulouse, Z. Zhang, C. B. Musgrave, and C. J. Umrigar, J. Chem. Phys. **131**, 124103 (2009).
[27] T. Bouabça, N. B. Amor, D. Maynau, and M. Caffarel, J. Chem. Phys. **130**, 114107 (2009).

[28]M. W. Schmidt, K. K. Baldridge, J. A. Boatz, S. T. Elbert, M. S. Gordon, J. H. Jensen, S. Koseki, N. Matsunaga, K. A. Nguyen, S. Su, T. L. Windus, M. Dupuis, and J. A. Montgomery, J. Comput. Chem. **14**, 1347 (1993).
[29]M. S. Gordon and M. W. Schmidt, in *Theory and Applications of Computational Chemistry: The First Forty Years*, edited by C. E. Dykstra, G. Frenking, K. S. Kim, and G. E. Scuseria (Elsevier Amsterdam, 2005), pp. 1167–1189.
[30]L. K. Wagner, M. Bajdich, and L. Mitas, J. Comput. Phys. **228**, 3390 (2009).
[31]A. D. Becke, J. Chem. Phys. **98**, 5648 (1993).
[32]P. J. Stephens, F. J. Devlin, C. F. Chabalowski, and M. J. Frisch, J. Phys. Chem. **98**, 11623 (1994).
[33]C. W. Greeff and W. A. Lester, Jr., J. Chem. Phys. **109**, 1607 (1998).
[34]I. Ovcharenko, A. Aspuru-Guzik, and W. A. Lester, Jr., J. Chem. Phys. **114**, 7790 (2001).
[35]T. H. Dunning, Jr., J. Chem. Phys. **90**, 1007 (1989).
[36]T. Tsuji, H. Takashima, H. Takeuchi, T. Egawa, and S. Konaka, J. Phys. Chem. A **105**, 9347 (2001).
[37]K. E. Schmidt and J. W. Moskowitz, J. Chem. Phys. **93**, 4172 (1990).
[38]C. J. Umrigar and C. Filippi, Phys. Rev. Lett. **94**, 150201 (2005).
[39]A. W. Adamson, A. Vogler, H. Kunkely, and R. Wachter, J. Am. Chem. Soc. **100**, 1298 (1978).
[40]J. P. Perdew, K. Burke, and M. Ernzerhof, Phys. Rev. Lett. **77**, 3865 (1996).
[41]J. P. Perdew, K. Burke, and M. Ernzerhof, Phys. Rev. Lett. **78**, 1396 (1997).
[42]J. Munkres, *Topology*, 2nd ed. (Prentice Hall, Englewood Cliffs, NJ, 1999).
[43]F. A. Reboredo and P. R. C. Kent, Phys. Rev. B **77**, 245110 (2008).
[44]R. Derian, M. Dubecký, I. Štich, and L. Mitas (unpublished).